STEM CELLS TRANSLATIONAL MEDICINE®

TISSUE-SPECIFIC PROGENITOR AND STEM CELLS

Transient Brown Adipocyte-Like Cells Derive from Peripheral Nerve Progenitors in Response to Bone Morphogenetic Protein 2

ELIZABETH A. SALISBURY,[a,b] ZAWAUNYKA W. LAZARD,[a] EROBOGHENE E. UBOGU,[c] ALAN R. DAVIS,[a,b,d,e] ELIZABETH A. OLMSTED-DAVIS[a,b,d,e]

Key Words. Adult stem cells • Brown fat • Bone • Cell migration • Gene delivery systems in vivo or in vitro • Bone morphogenetic protein 2 • Peripheral nerves • Perineurium • Beta-3 adrenergic receptor • Reelin

[a]Center for Cell and Gene Therapy, [b]Translational Biology and Molecular Medicine, [c]Department of Neurology, [d]Department of Pediatrics, and [e]Department of Orthopedic Surgery, Baylor College of Medicine, Houston, Texas, USA

Correspondence: Elizabeth A. Olmsted-Davis, Ph.D., Baylor College of Medicine, 1 Baylor Plaza, Alkek N1010, Houston, Texas 77030, USA. Telephone: 713-798-1230; Fax: 713-798-1253; E-Mail: edavis@bcm.edu

Received July 17, 2012; accepted for publication September 12, 2012; first published online in SCTM *EXPRESS* November 26, 2012.

©AlphaMed Press
1066-5099/2012/$20.00/0

http://dx.doi.org/10.5966/sctm.2012-0090

ABSTRACT

Perineurial-associated brown adipocyte-like cells were rapidly generated during bone morphogenetic protein 2 (BMP2)-induced sciatic nerve remodeling in the mouse. Two days after intramuscular injection of transduced mouse fibroblast cells expressing BMP2 into wild-type mice, there was replication of beta-3 adrenergic receptor$^+$ (ADRB3$^+$) cells within the sciatic nerve perineurium. Fluorescence-activated cell sorting and analysis of cells isolated from these nerves confirmed ADRB3$^+$ cell expansion and their expression of the neural migration marker HNK1. Similar analysis performed 4 days after BMP2 delivery revealed a significant decrease in ADRB3$^+$ cells from isolated sciatic nerves, with their concurrent appearance within the adjacent soft tissue, suggesting migration away from the nerve. These soft tissue-derived cells also expressed the brown adipose marker uncoupling protein 1 (UCP1). Quantification of ADRB3-specific RNA in total hind limb tissue revealed a 3-fold increase 2 days after delivery of BMP2, followed by a 70-fold increase in UCP1-specific RNA after 3 days. Expression levels then rapidly returned to baseline by 4 days. Interestingly, these ADRB3$^+$ UCP1$^+$ cells also expressed the neural guidance factor reelin. Reelin$^+$ cells demonstrated distinct patterns within the injected muscle, concentrated toward the area of BMP2 release. Blocking mast cell degranulation-induced nerve remodeling resulted in the complete abrogation of UCP1-specific RNA and protein expression within the hind limbs following BMP2 injection. The data collectively suggest that local BMP2 administration initiates a cascade of events leading to the expansion, migration, and differentiation of progenitors from the peripheral nerve perineurium to brown adipose-like cells in the mouse, a necessary prerequisite for associated nerve remodeling. STEM CELLS TRANSLATIONAL MEDICINE *2012;1:874–885*

INTRODUCTION

Studies examining the origins of brown adipose tissue (BAT) have suggested an embryonic Myf5-expressing precursor cell, which can give rise to either skeletal myoblasts or brown adipocytes, dependent on the expression of transcription factor PRDM16 [1, 2]. These studies also show that BAT induced by beta-3 agonists in white adipose tissue does not arise from the same progenitor as interscapular BAT, indicating diversity in the source of brown adipocytes. In addition to PRDM16, genes implicated in brown adipogenesis include peroxisome proliferator-activated receptor α (PPARα) [3], PPARγ coactivator 1α (PGC1α) [4], Dio2 [5], and FoxC2, which lead to the activation of the uncoupling protein 1 (UCP1) gene. UCP1 is a signature protein exclusive to brown adipocytes. It is the main effector of thermogenesis, capable of uncoupling oxidative phosphorylation to dissipate energy as heat [6, 7].

Generation of BAT, as well as its thermogenic functions, is controlled by activation of the sympathetic nervous system (SNS) [6, 8, 9]. Sympathetic nerves can be activated through local serotonin release during neurogenic inflammation (Fig. 1A) or systemically through the hypothalamus [10–12]. Binding of serotonin to the 5-hydroxytryptamine (5-HT) receptor leads to release of noradrenaline, which in turn stimulates beta-adrenergic receptor (ADRB) signaling pathways involved in the induction of BAT [13]. BAT is highly innervated by sympathetic nerves [14], and beta-3 agonists increase BAT in mice, dogs, primates, and adult humans [9, 15]. Excessive noradrenaline release, due to rare adrenal gland tumors (pheochromocytomas), is also associated with more abundant BAT in affected patients [9, 16].

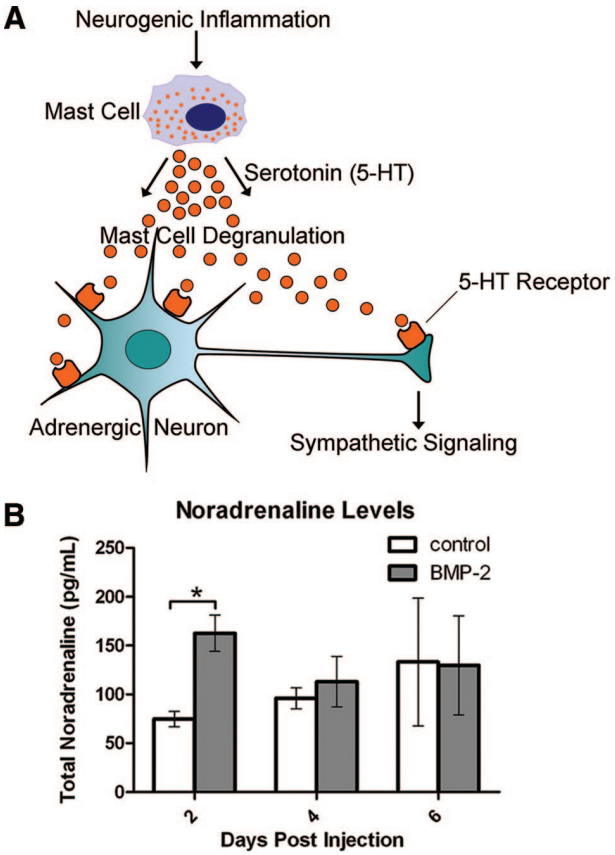

Figure 1. Analysis of sympathetic activity after exposure to BMP2. **(A):** Schematic of changes in sympathetic signaling induced by BMP2. BMP2-induced neurogenic inflammation leads to the recruitment and activation of mast cells. Upon activation, these mast cells degranulate, releasing serotonin that can then bind to its receptor on adrenergic neurons. This binding perpetuates downstream sympathetic signaling, including the release of noradrenaline. **(B):** Measurement of noradrenaline levels by enzyme-linked immunosorbent assay (ELISA) revealed a significant increase 2 days after delivery of AdBMP2 (BMP2) transduced cells, as compared to delivery of Adempty cassette (control) transduced cells. $n = 3$ biological replicates per time point. $*$, $p < .05$. Error bars represent $\pm$SEM. Abbreviations: BMP-2, bone morphogenetic protein 2; 5-HT, 5-hydroxytryptamine.

Although BAT depots play a critical role in adaptive thermogenesis [8, 9, 14], BAT is suggested to have other functions [17]. BAT is profoundly involved in triglyceride homeostasis [18] and controls microenvironmental oxygen tension enabling cartilage formation during endochondral ossification [17]. Intriguingly, astrocytes within the central nervous system (CNS) have been reported to express UCP1 and play a key functional role in the regulation of energy metabolism in the brain [19]. Our previous studies suggest that the robust aerobic respiration of brown adipocytes leads to the regulation of the local oxygen environment [17]. Interestingly, brown adipocytes also express vascular endothelial growth factor-A and -D (VEGF-A and -D) [20] and appear to regulate vessel formation. VEGF-D also has roles in lymphangiogenesis [21] and neuronal arborization [22], underscoring a potential role for brown adipocytes in coordinately orchestrating a multitude of regenerative tissue processes.

Although the production of brown adipose has been reported to be associated with activation of the SNS, the exact mechanism is unclear. We [23] and others [24] have shown that activation of sensory nerves, through bone morphogenetic protein 2 (BMP2), leads to the release of neuroinflammatory factors critical to this process [10] (Fig. 1A). Within 48 hours following delivery of BMP2-producing cells, peripheral nerve mast cells appeared to respond to the BMP2 and undergo degranulation [23], leading to the activation of matrix metalloproteinase 9 along the outer layers of adjacent peripheral nerves [25]. Simultaneous with these BMP2-induced changes within the nerves was the rapid appearance of brown adipocytes [17], suggesting a connection between nerve remodeling and brown adipogenesis.

Peripheral nerves possess a number of different cell populations, including stem/progenitor cells that exhibit plasticity [23, 26–28]. These cells have mainly been identified in the innermost compartment of peripheral nerves, the endoneurium, which contains the axons. This compartment is surrounded by a second region, known as the perineurium. The perineurium forms a physiological and structural barrier between the endoneurium and epineurium. This entire structure is supported by fibrous connective tissues known as the epineurium. These stringent neural barriers can be degraded as part of nerve remodeling, allowing the release of progenitors for tissue regeneration. Previous studies in our laboratory demonstrated peripheral nerve remodeling in response to BMP2 [23, 25].

The data presented here show the presence of a progenitor within peripheral nerves in the mouse that undergo rapid expansion, migration, and differentiation to brown adipocyte-like cells following local intramuscular BMP2 administration. These findings demonstrate the perineurium acts as a potential niche for progenitors in adult peripheral nerves, which are necessary for nerve remodeling associated with tissue regeneration. Furthermore, these nerve-derived brown adipocyte-like cells express a number of growth and patterning factors, as well as molecules that regulate oxygen utilization pathways, depending on their location within the tissue. Our observations support the notion that these brown adipocyte-like cells may orchestrate coordinated peripheral nerve regeneration or sprouting processes in adult mice.

Materials and Methods

BMP2 Delivery In Vivo

Replication-defective E1–E3 deleted first-generation human type 5 adenovirus possessing cDNA for BMP2 (AdBMP2) or no transgene (Adempty) was constructed as previously described [29]. Murine fibroblasts were transduced with either AdBMP2 or Adempty cassette control virus at a concentration of 5,000 viral particles per cell with 1.2% GeneJammer (details in [20, 29–31]).

The transduced cells were resuspended at a concentration of 5×10^6 cells per 100 μl of phosphate-buffered saline (PBS) and delivered through an intramuscular injection into the hind limb quadriceps muscle of C57/BL6 mice (Jackson Laboratory, Bar Harbor, ME, http://www.jax.org). Animals were euthanized at daily intervals after injection as indicated in the text. Hind limbs or sciatic nerves were harvested and either placed in formalin or snap frozen and stored at -80°C. All animal studies were performed in accordance with standards of the Department of Comparative Medicine of Baylor College of Medicine, after review and approval of the protocol by the Institutional Animal Care and Use Committee.

Cromolyn Administrations

Intraperitoneal injections of sodium cromoglycate (C0399; Sigma-Aldrich, St. Louis, MO, http://www.sigmaaldrich.com)

were administered daily (8 mg/kg per day) for 5 days prior to intramuscular injection of AdBMP2-transduced mouse fibroblasts and then continued daily, as previously described [23], until mice were euthanized at specified time points following BMP2 administration.

Quantification of Noradrenaline Levels

Blood was collected from animals ($n = 3$) receiving intramuscular injection of either AdBMP2 or Adempty transduced fibroblasts. Plasma was separated by centrifugation at 1,000*g* for 15 minutes at 4°C. Noradrenaline levels were assayed by enzyme-linked immunosorbent assay (catalog no. 40-734-35002; GenWay, San Diego, CA, http://www.genwaybio.com) according to the manufacturer's protocol. Sample analysis was done in duplicate, the results from each day following injection were averaged, and significance was evaluated by Student's *t* test.

Quantitative Real-Time Reverse Transcriptase Polymerase Chain Reaction

Total RNA from the entire hind limb soft tissues that received AdBMP2 or Adempty transduced cells were extracted using TRIzol Reagent (Life Technologies, Carlsbad, CA, http://www.lifetech.com) and purified using the Qiagen RNeasy Mini Kit, according to the manufacturer's protocol for RNA clean-up (Qiagen, Valencia, CA, http://www.qiagen.com). Soft tissues ($n = 4$) were collected every day for 6 days following injection. RNA integrity was confirmed by agarose gel electrophoresis, and concentrations were determined spectrophotometrically. The cDNA was synthesized from RNA using the RT^2 first strand kit (SA Biosciences Inc., Frederick, MD, http://www.sabiosciences.com). Real-time quantitative polymerase chain reaction (qPCR) analyses were done using the RT^2 qPCR Primer Assay (SA Biosciences) for ADRB3 (catalog no. PPM04810E-200), and UCP1 (catalog no. PPM05164A-200). For normalization, Tbp (TATA box binding protein; catalog no. PPM03560E-200) was found to be the best internal control. The RT^2 SYBR Green/ROX Master Mix (SA Biosciences) was used for polymerase chain reaction (PCR) amplification. The cDNA was subjected to quantitative real-time reverse transcriptase PCR analyses in parallel using a 7900HT PRISM Real-Time PCR machine and SDS 2.3 software (Applied Biosystems, Carlsbad, CA, http://www.appliedbiosystems.com). The Ct values, where Ct is defined as the threshold cycle of PCR at which cDNA reached exponential amplification, were determined for each biological sample in duplicate. Values were normalized against Tbp (TATA box binding protein), which was found to be independent of BMP2 (not shown) and expressed relative to RNA isolated from control tissues. Relative gene expression was determined using the $\Delta\Delta$Ct method, the experimental data at each time point were averaged, and the SEM was calculated. Statistical significance was evaluated by Student's *t* test. For comparison studies of RNA expression in cromolyn-treated mice treated with BMP2, relative gene expression was again determined using the $\Delta\Delta$Ct method, but in this instance relative to vehicle-treated animals treated with BMP2.

Isolation of Sciatic Nerve and Hind Limb Soft Tissue Cells

Sciatic nerves were dissected and cells isolated following previously described methods [32]. Briefly, sciatic nerves were dissected into cold Ca,Mg-free Hanks' balanced saline solution (HBSS) and dissociated by incubating for 4 minutes at 37°C in trypsin-versene (EDTA) diluted 1:10 in Ca,Mg-free HBSS, plus 0.25 mg/ml type 4 collagenase (Worthington Biochemical, Lakewood, NJ, http://www.worthington-biochem.com). After centrifugation, nerve-derived cells were triturated, filtered through nylon mesh, and resuspended in cell staining buffer (Biolegend, San Diego, CA, http://www.biolegend.com). Hind limb muscle tissue was dissected from the skeletal bone into cold HBSS and dissociated by mincing the tissues and incubating for 45 minutes at 37°C in 0.2% type 2 collagenase (Worthington) in HBSS. An equal volume of Dulbecco's modified Eagle's medium supplemented with 10% fetal bovine serum was added to quench the digestion reaction. Dissociated cells were centrifuged, triturated, filtered through nylon mesh, and resuspended in cell staining buffer. For each experiment, the sciatic nerves or muscles isolated from three mice (a total of six nerves or muscles) were pooled for further staining and fluorescence-activated cell sorting (FACS) analysis.

Flow Cytometry and FACS

Cells isolated from either the sciatic nerves or hind limb soft tissues were incubated with ADRB3 antibody (chicken polyclonal; 1:400 dilution; Abcam, Cambridge, MA, http://www.abcam.com) for 45 minutes on ice. Cells were washed with 1× PBS and then incubated with anti-chicken Alexa Fluor 488 (1:500 dilution; Invitrogen, Carlsbad, CA, http://www.invitrogen.com) for 30 minutes on ice. Cells were again washed with 1× PBS, and stained cells were analyzed on a FACSAria II (Becton, Dickinson and Company, Mountain View, CA, http://www.bd.com) flow cytometer and BD FACSDiva software. For dual-antibody labeling, isolated cells were also incubated with HNK1 antibody (rabbit polyclonal; 1:40 dilution; Bioss, Woburn, MA, http://www.bioss-usa.com) and the respective secondary. For cell sorting, labeled cells were separated based on their fluorescence intensity, and the ADRB3-negative and -positive populations were collected with >95% purity. The percentage of positive cells from each experiment was averaged, the SEM was calculated, and statistical significance evaluated by Student's *t* test.

Immunohistochemical and Immunocytochemical Analysis

Mouse hind limbs were isolated, formalin fixed, decalcified, and processed for paraffin sectioning. Prior to sectioning, the tissues were cut longitudinally and both halves embedded so that the tissues were sectioned from the inside outward as previously described [17]. Serial sections were prepared (5 μm), and every fifth section was mounted on a slide and stained with hematoxylin and eosin. Unstained serial sections were processed for immunohistochemistry (either single- or double-antibody labeling), using methods described previously [17]. Briefly, for indirect immunofluorescence staining, sections were incubated with primary antibodies, followed by washing and incubation with respective secondary antibodies, used at 1:500 dilution, to which Alexa Fluor 488, 594, or 647 (Invitrogen) was conjugated. Primary antibodies were used as follows: UCP1, rabbit polyclonal, 1:200 dilution (Chemicon, Temecula, CA, http://www.chemicon.com); ADRB3, rabbit polyclonal, 1:100 dilution (Cell Applications Inc., San Diego, CA, http://www.cellapplications.com); neurofilament, mouse monoclonal, 1:200 dilution (Sigma-Aldrich); Ki67, rat monoclonal, 1:50 dilution (Dako, Carpinteria, CA, http://www.dako.com); HNK1, mouse monoclonal, 1:15 dilution (Becton Dickson); beta-1,3-glucuronyl transferase 2

(B3GAT2), goat polyclonal, 1:50 dilution (Santa Cruz Biotechnology Inc., Santa Cruz, CA, http://www.scbt.com); and reelin, mouse monoclonal, 1:500 dilution (Abcam). Primary and secondary antibodies were diluted in 2% bovine serum albumin (BSA) or, for mouse primary antibodies, staining was performed using the Mouse on Mouse (M.O.M.) kit (Vector Laboratories, Burlingame, CA, http://www.vectorlabs.com) according to the manufacturer's protocol. Tissues were counterstained and covered with Vectashield mounting medium containing 4′,6-diamidino-2-phenylindole (DAPI) (Vector Laboratories). When sections were stained using horseradish peroxidase, they were processed using the PowerVision Poly-HRP Anti-Rabbit IHC Detection System (Leica Microsystems, Buffalo Grove, IL, http://www.leica.com) according to the manufacturer's instructions and were counterstained with hematoxylin.

Mouse sciatic nerves were frozen sectioned longitudinally and fixed with 4% paraformaldehyde in 1× PBS, washed in PBS, and permeabilized with 0.3% Triton X-100 in Tris-buffered saline. They were then stained following the indirect immunofluorescence protocol described above.

Cytospin slide preparations of FACS isolated cells were produced by centrifugation of approximately 40,000 cells at 500 rpm, using a Cytopro 7620 cytocentrifuge (Wescor, Logan, UT, http://www.wescor.com), for 5 minutes. The slides were subsequently immunostained following similar methods as above. Briefly, cells were fixed with 4% paraformaldehyde, PBS-washed, treated with 0.3% Triton X-100 in 0.3% Tris-buffered saline, blocked with 2% BSA, and incubated in primary antibody overnight. After PBS washing, samples were incubated in the appropriate secondary antibody and counterstained with DAPI. Stained cells were examined by confocal microscopy (LSM 510 META; Zeiss, Inc., Thornwood, NY, http://www.zeiss.com).

Statistical Analysis

Data are expressed as mean ± SEM. Statistical significance was determined by Student's *t* test, with $p < .05$ considered significant.

Results

Upregulation of Sympathetic Activity Prior to Induction of BAT After Exposure to BMP2

One of the first steps in SNS signaling is the release of noradrenaline, which is synthesized and released by noradrenergic nerves (Fig. 1A). Therefore, we measured the levels of this hormone after exposure to BMP2. We observed a significant increase ($p < .05$) in circulating noradrenaline levels in mice receiving the AdBMP2-transduced fibroblasts, as compared with controls receiving Adempty-transduced cells, 2 days following induction (Fig. 1B). The data suggest early enhanced SNS activity following BMP2 stimulation.

Expansion of ADRB3$^+$ Cells Localized Within Peripheral Nerve Perineurium After Exposure to BMP2

To determine what cells within the skeletal muscle possess adrenergic receptor, mouse hind limbs receiving either AdBMP2- or Adempty-transduced cells were isolated at 1 and 3 days after injection, serially sectioned, and then immunostained for ADRB3$^+$ expression (Fig. 2A). The patterns of ADRB3$^+$ immunostaining in tissues isolated from mice after 1 day of exposure to the AdBMP2-transduced cells were similar to those of the control tissues or those receiving Adempty-transduced cells. In both tissues, positive expression of this receptor (Fig. 2A, green) was observed on rare cells within the endoneurium and perineurium of peripheral nerves. The endoneurium is indicated in Figure 2A by the detection of axons by the neurofilament antibody (red). However, 3 days after receiving AdBMP2-transduced cells, ADRB3$^+$ cells were found predominantly in a thickened layer surrounding the nerve (consistent with the perineurium), as well as within the skeletal muscle (Fig. 2A).

To determine whether these ADRB3$^+$ cells were replicating, tissues were coimmunostained with the antibody Ki-67 (Fig. 2A, red) [33]. In the control tissues, as well as those isolated 1 day after BMP2 delivery via AdBMP2 transduced fibroblasts, the rare ADRB3$^+$ cells were quiescent (Fig. 2A). However, 3 days after the initial delivery of BMP2, a large number of the ADRB3$^+$ cells surrounding or extending from the peripheral nerve appeared to be replicating. Interestingly, the majority of ADRB3$^+$ cells observed between the skeletal muscle fibers were not replicating, based on lack of Ki-67 detection (Fig. 2A). The data suggest that ADRB3$^+$ cells associated with peripheral nerves may undergo rapid expansion after exposure to BMP2.

Quantification of ADRB3$^+$ Cells After Exposure to BMP2 Reveals a Major Shift in the Location of These Cells

Since immunohistochemical staining for ADRB3 suggested that these cells were more abundant following BMP2 administration, we quantified the ADRB3$^+$ cells in the hind limb soft tissues isolated 2, 3, and 4 days after delivery of AdBMP2-transduced fibroblasts, using FACS analysis (Fig. 2B). As expected from the immunostaining, the number of ADRB3$^+$ cells was identical to the control on day 2 (Fig. 2B) but then significantly increased ($p < .05$) on days 3 and 4, as compared with either the number of cells on day 2 after receiving AdBMP2-transduced cells or any of the control tissues (Fig. 2B). We did not observe ADRB3$^+$ expression in our transduced mouse fibroblasts (data not shown).

To determine whether the increase was occurring within the population of cells associated with peripheral nerves, we isolated the sciatic nerve and immunostained to confirm that the ADRB3$^+$ population was both a component of the nerve and expanding as seen in the nerves in the whole tissue sections. As seen in Figure 2C, there was extensive ADRB3$^+$ staining along the outer layer of the nerve fascicle, which also stained positively for Ki-67 2 days after BMP2 induction. ADRB3$^+$ cells were present within the sciatic nerves, with expression predominantly within the perineurium at rest and following BMP2 induction.

Quantification through FACS showed a trend toward an increase in ADRB3$^+$ cells associated with the sciatic nerves isolated 2 days following BMP2 administration (Fig. 2D). Surprisingly, in tissues isolated 4 days after BMP2 induction, there was a dramatic decrease ($p < .005$) in ADRB3 expression in the total nerve-associated cell population as compared with control nerve tissues (Fig. 2D). These data suggest that peripheral nerve-derived ADRB3$^+$ cells expand after exposure to BMP2 for 48 hours but then disappear from the nerve completely by 4 days, temporally associated with the peak expression in the local soft tissues, including skeletal muscle (compare Fig. 2B and 2D). We hypothesize that the increase in ADRB3$^+$ cells within the hind limb soft tissues is due to expansion and migration of the perineurial-associated cells.

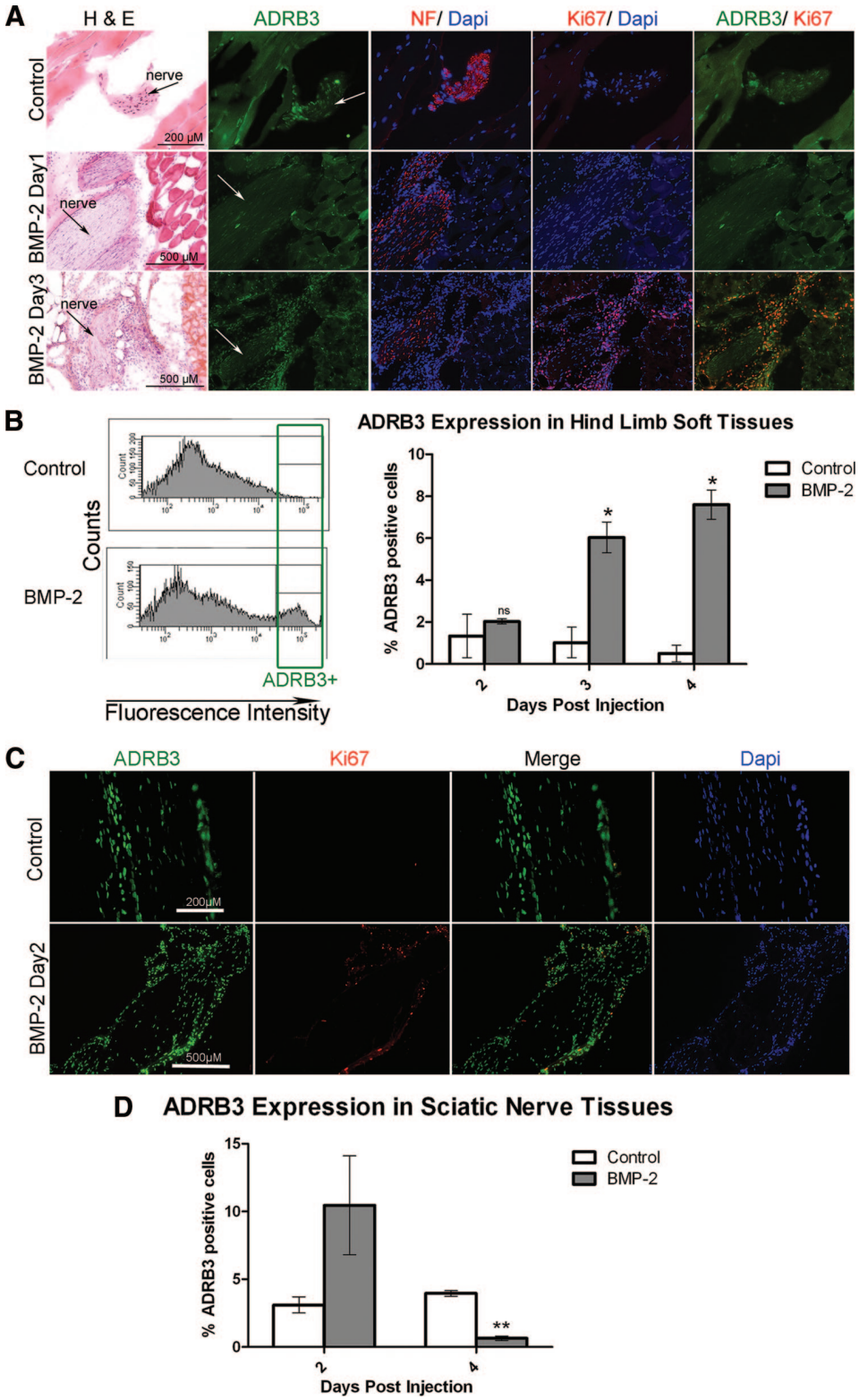

Figure 2. Activation of ADRB3$^+$ cells associated with the peripheral nerve perineurium after exposure to BMP2. **(A):** Representative photomicrographs of ADRB3 expression within the soft tissues of the hind limb showed ADRB3$^+$ cells undergoing replication in the perineurial region of the peripheral nerves 3 days after delivery of AdBMP2 transduced cells. Shown are ADRB3 (green), neurofilament (red), and Ki67 (red) in the rightmost column. Arrows indicate the nerves. **(B):** Flow cytometric analysis of ADRB3 expression within the soft tissues of the hind limb revealed a significant increase in the number of ADRB3$^+$ cells after 3 and 4 days of exposure to BMP2. A representative histogram of the percentage of ADRB3$^+$ cells on day 4 is shown. **(C):** Representative photomicrographs of ADRB3 expression within the sciatic nerve tissues showed ADRB3$^+$ cells associated with the perineurium and coexpressing the proliferation marker Ki67, 2 days after delivery of AdBMP2 transduced cells. Tissues were counterstained with Dapi (blue). Shown are ADRB3 (green) and Ki67 (red). **(D):** Flow cytometric analysis of ADRB3 expression within the sciatic nerve

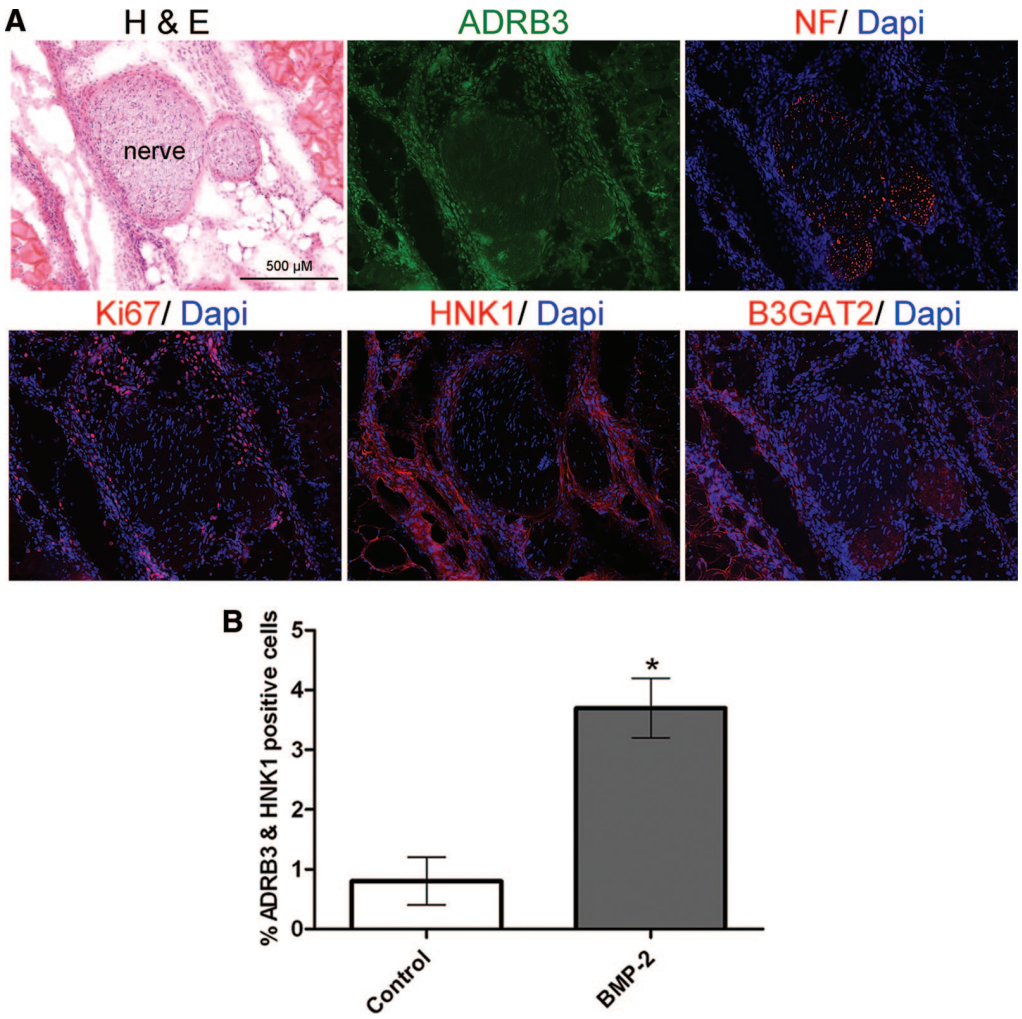

Figure 3. Analysis of expression of the neural migratory marker HNK1 after induction with BMP2. **(A):** Representative photomicrographs of the HNK1 staining pattern in serial sections from the soft tissues of the hind limb, 3 days after delivery of AdBMP2 transduced cells. Again, note the ADRB3$^+$ cell population associated with the nerves, which is replicating and overlapping expression of the migratory markers. Shown are ADRB3 (green), NF (red, top), Ki67 (red, bottom left), HNK1 (red, bottom center), and B3GAT2 (red, bottom right) Scale bar = 500 μm. **(B):** Flow cytometric analysis for dual expression of ADRB3 and HNK1 after 4 days of exposure to BMP2. $n = 3$. $*$, $p < .05$. Error bars represent $\pm$ SEM. Abbreviations: ADRB3, beta-3 adrenergic receptor; B3GAT2, beta-1,3-glucuronyl transferase 2; BMP, bone morphogenetic protein; Dapi, 4′,6-diamidino-2-phenylindole; H&E, hematoxylin and eosin; NF, neurofilament.

ADRB3$^+$ Cells Replicate and Migrate from the Nerve

To determine whether these cells could potentially migrate from peripheral nerves, we next immunostained (Fig. 3A) for the neuronal migratory marker HNK1 [34–36]. Serial sections generated from soft tissue of the hind limb, isolated 3 days after BMP2 delivery, showed ADRB3$^+$ (Fig. 3A, green) cells undergoing replication (Ki67; red). These cells also appeared to possess the carbohydrate epitope HNK1 (Fig. 3A, red) and were found in tissues surrounding and extending from peripheral nerves, as determined by neurofilament staining (red). These cells were HNK1-negative in control tissues or those receiving the Adempty control cells (not shown). The HNK1 carbohydrate moiety is generated through activation of B3GAT2, specifically activated in migratory neural stem cells [37]. Immunohistochemical staining demonstrated B3GAT2 expression by peripheral nerves, appearing in the same general pattern as HNK1 expression.

To quantify the increased cellular expression of HNK1 after exposure to BMP2 and confirm coexpression with ADRB3$^+$, cells isolated from hind limb soft tissue 4 days after receiving AdBMP2-transduced cells were examined by flow cytometry. In these comparison studies, there was a significant ($p < .05$) increase in the number of ADRB3$^+$ cells that also expressed HNK1 following BMP2 induction compared with controls (Fig. 3B). The data collectively suggest that BMP2 may trigger replication and migration of ADRB3$^+$ cells in the perineurium from nearby peripheral nerves.

tissues revealed a marked increase in the number of ADRB3$^+$ cells after 2 days of exposure to BMP2, followed by a significant decrease after 4 days. For each experiment, six hind limb or nerve samples for each condition were pooled for flow cytometric analysis. Bar graphs show the average of three independent experiments $\pm$ SEM. $*$, $p < .05$; $**$, $p < .005$. Abbreviations: ADRB3, beta-3 adrenergic receptor; BMP-2, bone morphogenetic protein 2; Dapi, 4′,6-diamidino-2-phenylindole; H&E, hematoxylin and eosin; NF, neurofilament; ns, not significant.

ADRB3$^+$ Cells Differentiate into Brown Adipocytes

Immunohistochemical staining of serial tissue sections suggested that UCP1$^+$ brown adipocyte-like cells previously observed following BMP2 induction may be the ADRB3$^+$ cells migrating from peripheral nerves (Fig. 4A, brown). Serial sections generated from isolated sciatic nerves and immunostained for UCP1 and ADRB3 also demonstrated perineurial and endoneurial cellular coexpression (Fig. 4B).

To further confirm that ADRB3$^+$cells express UCP1, cells were isolated from hind limb soft tissue near the site of injection 4 days after exposure to BMP2 and sorted by FACS. ADRB3$^+$ and ADRB3$^-$ cell populations were cytospun onto slides and then immunostained for ADRB3 and UCP1. The results, depicted in Figure 4C, show that all ADRB3$^+$ cells analyzed expressed UCP1. Furthermore, UCP1 expression was not observed in the ADRB3$^-$ population. Collectively, the data suggest that murine ADRB3$^+$ cells residing within peripheral nerves undergo expansion by replication predominantly within the perineurium, migrate from peripheral nerves into surrounding soft tissues including skeletal muscle, and differentiate toward a brown adipocyte phenotype in response to BMP2.

Certain BAT-Specific RNAs (ADRB3 and UCP1) Are Transiently Elevated After BMP2 Induction, but Not Others (PRDM16 and PPARγ)

To further characterize the brown adipocyte phenotype, we used quantitative real-time PCR to detect ADRB3 and UCP1-specific RNA expression. RNA was isolated from hind limb soft tissues 1–6 days after injection of AdBMP2- or Adempty-transduced cells. As expected, there was a significant increase ($p < .05$) in ADRB3-specific RNA 2 days after BMP2 induction compared with negative controls (Fig. 4D). Furthermore, UCP1-specific RNA was dramatically elevated on both days 2 and 3, with a greater than 70-fold increase on day 3 ($p < .0005$) that fell to basal levels on day 4 (Fig. 4E).

Although ADRB3 is the most predominant effector of adrenergic stimulated BAT biogenesis, beta-2 adrenergic receptor may also participate [8, 38]. We did not observe a significant change in ADRB2-specific RNA in the soft tissues of mice following BMP2 induction relative to controls (supplemental online Fig. 1A). Surprisingly, we also did not observe significant changes in expression of genes previously associated with BAT biogenesis, including PRDM16, PPARγ, PPARα, and PPARδ (supplemental online Fig. 1B–1E, respectively). There was a trend toward early PGC1α expression following BMP2 induction (supplemental online Fig. 1F), which follows our previous findings that linked expression of this protein with the brown adipose tissue [17]. The data suggest that these brown adipocyte-like cells may be a transient or specialized form of BAT that can be rapidly generated by exposure to BMP2.

BAT-Like Cells Express Reelin

Nerve remodeling and extension, in the CNS, involves the expression and regulation of the neural guidance factor reelin, occurring simultaneously with the expression of UCP1 [19, 39, 40]. We sought to determine whether brown adipocyte-like cells express reelin. Figure 5A shows expression of reelin in cells in the endomysium between the muscle fibers in distinct patterns or aggregates of cells running from peripheral nerves to the area where the AdBMP2-transduced cells reside. Reelin expression (red) colocalized to a subset of ADRB3 expressing cells (green), suggesting that as the ADRB3$^+$ cells migrate they may undergo differentiation (Fig. 5A). To confirm the coexpression of these proteins identified by immunohistochemistry, ADRB3$^+$ cells were isolated from hind limb soft tissues by FACS 4 days after BMP2 induction, followed by cytospin analysis (Fig. 5B). Four-color confocal microscopy showed coexpression of all three markers (UCP1, reelin, and ADRB3) by a subset of these isolated cells. Analysis indicated that almost all ADRB3$^+$ cells expressed UCP1, but not all ADRB3$^+$ cells expressed reelin (data not shown). The data suggest that brown adipocyte-like differentiation may result in different phenotypes depending on the location of the ADRB3$^+$ cells within the tissues following BMP2 induction in mice.

Inhibition of the Sympathetic Pathway by Blocking Mast Cell Degranulation Suppresses Induction of BAT-Like Cells

We hypothesize that mast cell degranulation releases factors and proteinases [25] that promote perineurial layer alterations that facilitate the release of cells. Therefore, blocking mast cell degranulation should suppress SNS signaling, nerve remodeling, and brown adipogenesis following BMP2 induction (Fig. 1A). To test this, we inhibited mast cell degranulation and examined changes in ADRB3 and UCP1-specific RNA within the hind limb soft tissues. Mice were pretreated with either sodium cromoglycate (cromolyn), a known inhibitor of mast cell degranulation [41], or a vehicle control (PBS). Relative RNA expression was quantified at specific time points after delivery of AdBMP2-transduced fibroblasts. The results indicate that there was a significant decrease ($p < .05$) in both the ADRB3 and UCP1-specific RNA expression following cromolyn treatment, compared with vehicle-treated mice (Fig. 6A).

The results suggest that ADRB3$^+$ cells neither replicate, migrate, nor undergo brown adipogenesis in the presence of cromolyn. To confirm this, cromolyn- or vehicle-treated hind limb soft tissues were isolated 2 days after BMP2 induction and immunostained for UCP1. As seen in Figure 6B, there was a dramatic absence of UCP1$^+$ cells (green) in tissue sections generated from mice pretreated with cromolyn, either associated with the nerve or throughout the surrounding soft tissue, including skeletal muscle. This was in contrast to the vehicle-treated animals (Fig. 6B). These data further implicate a mechanism by which mast cell degranulation and sympathetic activation are important for the production of brown adipocyte-like cells, derived from the perineurium and endoneurium of peripheral nerves in the mouse.

Discussion

The results presented here demonstrate the presence of a unique brown adipocyte-like progenitor cell that resides within the mouse peripheral nerve perineurium and endoneurium and responds to local BMP2 administration by replication, migration, and differentiation. Unlike its human counterpart, the mouse sciatic nerve mainly consists of a single fascicle surrounded by its perineurium. The epineurium is loosely associated with the nerve. The perineurium consists mainly of specialized epitheloid myofibroblasts through which epineurial arterioles and postcapillary endoneurial venules traverse. The perineurium and endoneurial microvessels possess restrictive tight junctions and form the blood-nerve interface, which is necessary for maintaining the internal homeostasis in peripheral nerves [42]. Although Schwann cells from the endoneurium may traffic through the

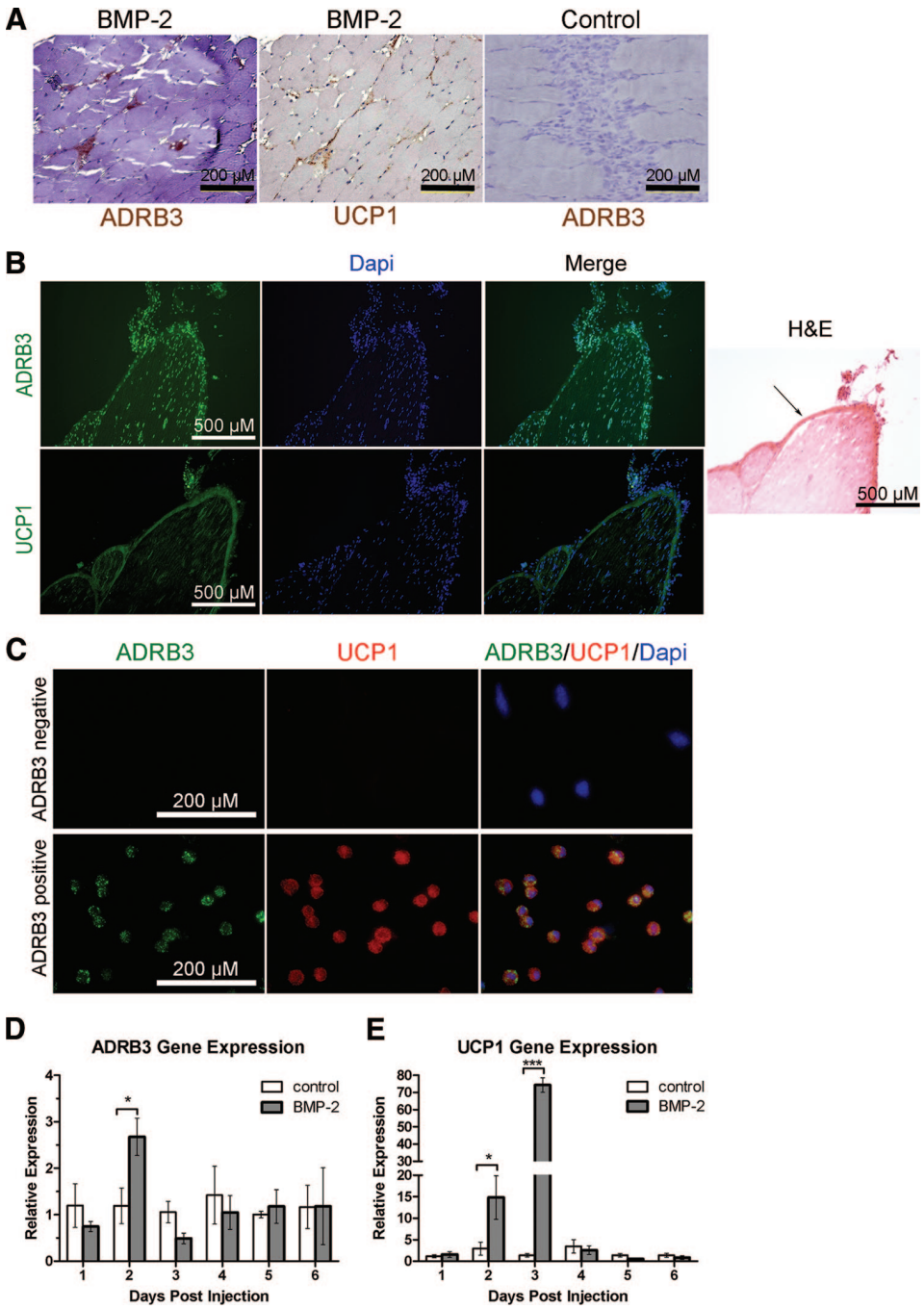

Figure 4. ADRB3^{+} cells activated by BMP2 also express the brown adipocyte marker UCP1. **(A):** Representative photomicrographs of hind limb tissues isolated 4 days after delivery of AdBMP2 transduced cells showed ADRB3 staining (brown), which coaligns with UCP1 staining (brown) on an adjacent serial tissue section. This staining was not seen in hind limb tissues isolated 4 days after delivery of Adempty (control) transduced cells. Scale bars = 200 μm. **(B):** Sciatic nerve tissues isolated 2 days after BMP2 induction showed ADRB3 staining (green, top), which coaligns with UCP1 staining (green, bottom) on an adjacent serial tissue section. Tissues were counter-stained with Dapi (blue). H&E-stained sections from the same tissue are shown. Arrow indicates the perineurium. Scale bars = 500 μm. **(C):** ADRB3^{+} and ADRB3^{-} cell populations from the soft tissues of the hind limb were isolated by fluorescence-activated cell sorting after 4 days of exposure to BMP2. Cytospin preparations of the sorted cells were immunostained and showed colocalization of UCP1 (red) and ADRB3 (green). Scale bars = 500 μm. **(D, E):** Quantitative real-time reverse transcriptase polymerase chain reaction analysis showed an increase in ADRB3 and UCP1 RNA levels after 2 days of exposure to BMP2. Relative gene expression is represented in relation to control tissues from animals injected with Adempty-transduced cells using the $\Delta\Delta$Ct method. $n = 4$. *, $p < .05$; ***, $p < .0005$. Error bars represent $\pm$SEM. Abbreviations: ADRB3, beta-3 adrenergic receptor; BMP, bone morphogenetic protein; Dapi, 4′,6-diamidino-2-phenylindole; H&E, hematoxylin and eosin; UCP1, uncoupling protein 1.

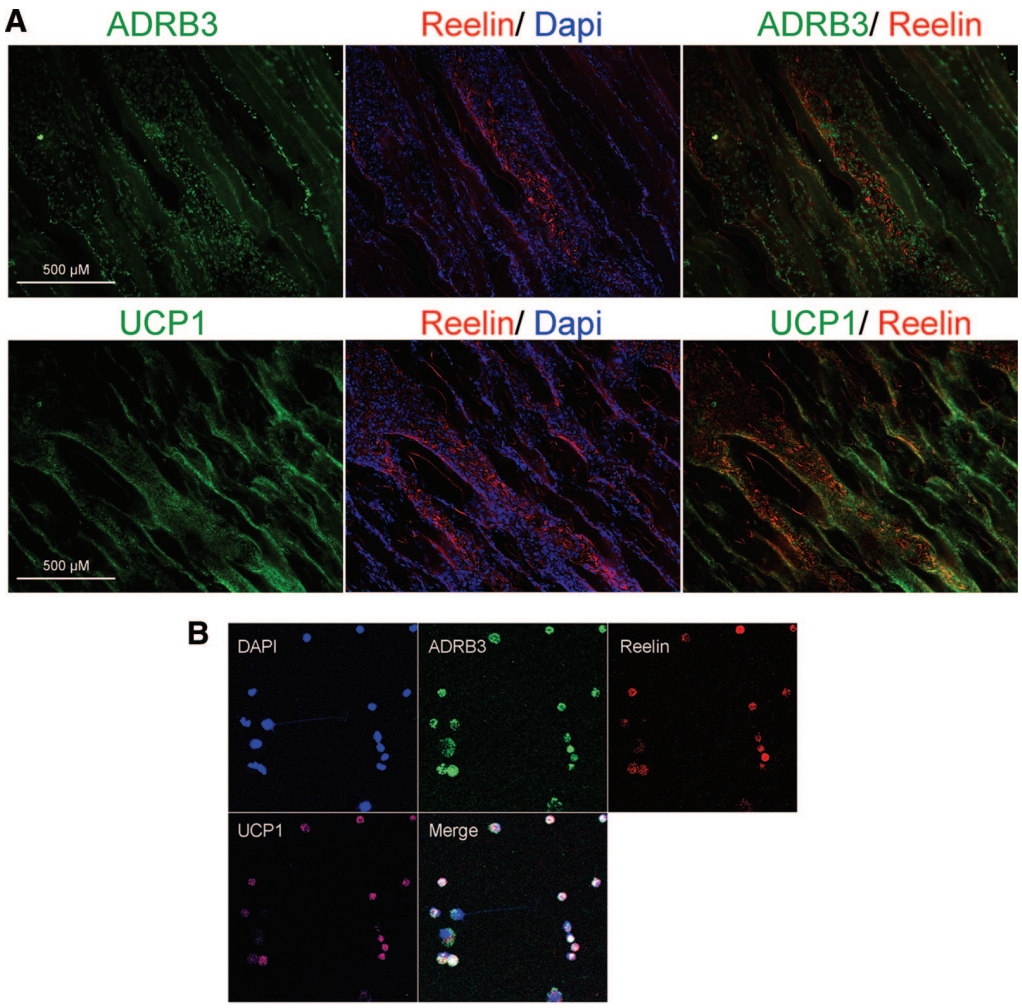

Figure 5. Transient brown adipocyte-like cells express reelin. **(A):** Representative photomicrographs of reelin (red), ADRB3 (green, top), and UCP1 (green, bottom) expression 4 days after delivery of AdBMP2 transduced cells. Tissues were counterstained with Dapi (blue). Scale bars = 500 μm. **(B):** ADRB3$^+$ cells from the soft tissues of the hind limb were isolated by fluorescence-activated cell sorting after 4 days of exposure to BMP2. These cells were centrifuged on slides and labeled with ADRB3 (green), reelin (red), or UCP1 (pink). Each field is 0.050625 mm^2. Abbreviations: ADRB3, beta-3 adrenergic receptor; Dapi, 4′,6-diamidino-2-phenylindole; UCP1, uncoupling protein 1.

perineurium as they migrate during axonal sprouting and growth, the unique pattern of ADRB3 expression, even in a resting state, suggests that the progenitors described here are predominantly resident within the perineurium.

Morrison et al. [43] demonstrated the presence of a neural crest-derived cell localized to the boundary between the endoneurium and perineurium in mice. They also demonstrated the presence of desert hedgehog-expressing cells derived from neural crest stem cells that serve as progenitors for both Schwann cells and endoneurial fibroblasts [44]. Interestingly, it has been demonstrated that the deletion of Nf1 must occur at exactly embryonic day 12.5 and not before (neural crest stem cells) or after (mature Schwann cells) for neurofibromas to occur in mouse models of neurofibromatosis [45]. Since both endoneurial fibroblast and Schwann cell progenitors express desert hedgehog, a branch in their differentiation is likely to occur after this point. We speculate that the endoneurial fibroblasts may be the progenitor for the ADRB3$^+$ perineurial cell, since it has previously been proposed that endoneurial fibroblasts are the progenitors for perineurial cells. However, the origin of perineurial cells remains a challenging question. A recent study demonstrated that motor axon-ensheathing cells (termed perineurial glia) in zebrafish were derived from migratory CNS glia [46]. This is in contrast to rat fetal in vitro studies that suggested that fibroblasts, which were derived from cranial periosteum, were responsible for perineurial sheath development when cocultured with axons and Schwann cells [47].

Although rare ADRB3$^+$ cells are normally present in peripheral nerves in mice, these cells rapidly expand in the presence of BMP2. We have previously determined that the AdBMP2-transduced fibroblasts express levels of BMP2 (approximately 20 ng per day) that are generated physiologically during fracture [48]. These cells survive in the tissue at the injection site for approximately 6 days. Although the cells had been transduced with an adenovirus containing the BMP2 cDNA, control mice were treated with cells transduced with an adenovirus vector containing the same adenovirus backbone but lacking the BMP2 transgene cassette. Therefore, the difference in results between BMP2-induced mice and controls is due to BMP2 expression. Consistent with this is the observation that mice receiving cells

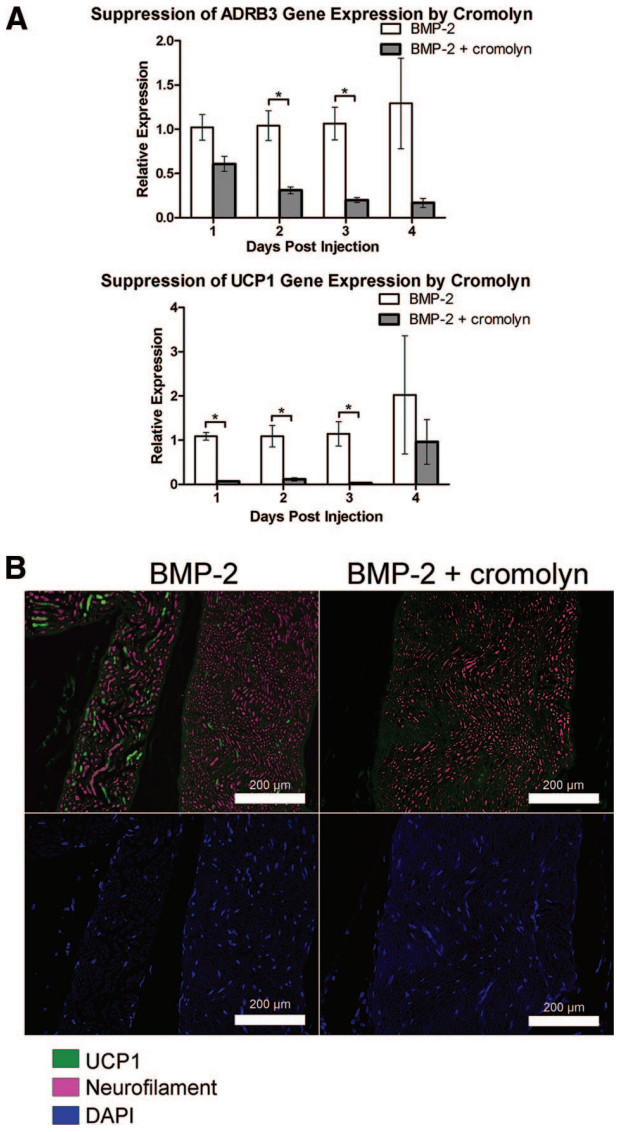

Figure 6. Suppression of induction of brown adipocyte-like cells in the presence of cromolyn, an inhibitor of mast cell degranulation. **(A):** RNA was isolated from the hind limb soft tissues of animals after BMP2 delivery and pretreatment with either cromolyn (BMP2 + cromolyn) or a vehicle control for drug delivery (BMP2). Relative gene expression in animals treated with BMP2 and cromolyn was expressed in relation to animals treated with BMP2 alone (vehicle-treated animals) using the $\Delta\Delta$Ct method. Quantitative real-time reverse transcriptase polymerase chain reaction analysis showed suppression of both ADRB3 and UCP1 relative gene expression in the cromolyn-treated animals, with a 39-fold suppression of UCP1 on day 3. $n = 4$. $*$, $p < .05$. Error bars represent $\pm$SEM. **(B):** Representative photomicrographs of UCP1 (green) expression within the hind limb soft tissues 2 days after injection of BMP2 transduced cells in animals treated with cromolyn (BMP2 + cromolyn) or left untreated, receiving only vehicle (BMP2). Neurofilament (pink) marks the nerves. Tissues were counterstained with Dapi (blue). Scale bars = 200 μm. Abbreviations: ADRB3, beta-3 adrenergic receptor; BMP, bone morphogenetic protein; DAPI, 4′,6-diamidino-2-phenylindole; UCP1, uncoupling protein 1.

transduced with the control virus yielded results similar to those found in mice that received no injection in all cases. These data indicate that BMP2, directly or indirectly, leads to expansion of ADRB3$^+$ cells. Previous studies suggest that BMP2 asserts direct effects on peripheral nerves, leading to release of inflammatory mediators substance P and calcitonin gene-related peptide [49]. Therefore, we hypothesize that the effect of BMP2 on the activation of brown adipocyte-like cell progenitors may be indirect. In support of this, preadministration of cromolyn to inhibit mast cell degranulation suppressed this process. By inhibiting mast cell degranulation, stored serotonin is not released, preventing expression of noradrenaline. Furthermore, blockade of mast cell chymase and protease release will prevent peripheral nerve remodeling and inhibit release of ADRB3$^+$ cells to surrounding soft tissues.

In the presence of BMP2, ADRB3$^+$ cells replicate, as determined by positive staining with the Ki-67 antibody. A significant increase was observed in ADRB3-specific RNA, suggesting an increase in ADRB3$^+$ cell number, ADRB3-specific gene expression, or both. Interestingly, ADRB3 expression was observed in a significant number of cells trafficking between the muscle fibers 3–4 days after induction with BMP2. However, these cells were not replicating, suggesting that at this stage the cells are undergoing differentiation. Supporting the notion that the ADRB3$^+$ cells within muscle endomysium (i.e., between muscle fibers) arise from a replicating neuronal cell population is the steep decline of nerve-associated ADRB3$^+$ cells several days following BMP2 induction, with the population being significantly lower than at a resting state. In further support of the idea that these cells are migrating into the soft tissues is the presence of the carbohydrate moiety HNK1, which has been shown to be essential for neural stem cell migration [50, 51].

Previous research has established SNS control, via noradrenaline release and adrenergic receptor stimulation, of the proliferation, differentiation, and activity of classic, resident BAT [6, 8]. Here we show an increase in circulating noradrenaline within 2 days after intramuscular delivery of AdBMP2-transduced fibroblasts. Temporally associated with increased noradrenaline, ADRB3$^+$ cells coexpressed the brown adipocyte marker UCP1, and such expression was not observed in untreated or control mice. The induction of UCP1 in ADRB3$^+$ cells following BMP2 stimulation is supported by the large (70-fold) change in UCP1-specific RNA level. This rapid induction suggests that peripheral nerve-associated ADRB3$^+$ cells may serve as progenitors undergoing differentiation into brown adipocyte-like cells. However, interscapular BAT, as well as BAT derived from white fat, appears to have significant differences. The brown adipocyte-like cells derived from ADRB3$^+$ cells appear to be rapidly generated, but intriguingly, UCP1-specific RNA expression then rapidly drops to control levels, suggesting that this phenotype is transiently present. Also, substantial differences appear to be present in the biogenesis of these brown adipocyte-like cells, since after BMP2 induction there was a lack of significant change in the levels of RNA specific for either PPARγ, which is a central regulator of adipogenic differentiation [52, 53], or PRDM16, which controls the development of brown adipocytes in traditional BAT depots [1, 54]. Finally, it has been previously noted that mice lacking PPARγ still expresses UCP1 in brown adipose tissue. It was suggested that PGC1α coactivates other transcription factors (including PPARα); thus, the significance of PPARγ for the physiological control of UCP1 gene expression is not settled even in BAT found in traditional depots [53]. These differences suggest that there may be different molecular pathways and sources for cells with the brown adipocyte phenotype in adult organisms, as compared with BAT depots established embryonically. Alternatively,

this could suggest that these cells express some functional properties similar to BAT but are a distinct cell type.

One surprising finding in these studies is the expression of reelin in a subset of these brown adipocyte-like cells. Reelin is responsible for the "reeling gait" caused by the profound cerebellar hypoplasia in the *Reeler* mouse [55, 56]. Recently, reelin expression by astrocytes in the central nervous system has been demonstrated. Reelin functions as a critical factor in determining the positional identity of these cells [57]. Astrocytes play a key role in the regulation of neuronal energy metabolism in the brain, and PCG1α has recently been found to be a key regulator of astrocyte mitochondria (reviewed in [19]). The brown adipocyte-like cells described in this report may perform a similar function in neurometabolic coupling during peripheral nerve remodeling, to ensure that other cells induced by BMP2 receive the proper supply of oxygen and energetic metabolites (reviewed in [58]). The fact that the cell we have termed a "BAT-like cell" is an energy powerhouse [17], is intimately associated with the vasculature [20], and expresses the key neural guidance molecule reelin suggests that it may have an essential function in peripheral nerves similar to the role of astrocytes in the brain.

Conclusion

In this study, we found that ADRB3$^+$ cells expand and migrate following a local increase in BMP2 levels. It is intriguing to note that enhanced BMP-dependent signaling occurs in many cases of tissue injury or disease, involving blood vessels [59], muscle [60], and bone [23, 61], indicating that these cells may have implications in a variety of pathological processes. Our data also suggest that these cells are normally resident in peripheral nerves and may play important roles in inducing and guiding nerve remodeling during repair. This is the first report of a unique progenitor cell present predominantly within the perineurium of adult mouse peripheral nerves. Additional studies are needed to further characterize these cells and decipher their roles in heterotopic ossification, as well as the maintenance and repair of peripheral nerves.

Our discovery of progenitors for brown adipocyte-like cells in the perineurium of peripheral nerves has several clinical implications. First, neurofibroma tumor formation in the disease neurofibromatosis type I occurs within the perineurium [62]. These brown adipocyte-like cells that reside in the perineurium may be a component of this tumor or may aid in tumor formation through their ability to direct the formation of new nerves and vessels for possible innervation and vascularization of the growing tumor. In addition, our findings of brown adipocyte-like cells that regulate energy metabolism and potentially have a role in nerve remodeling could have relevance for neuronal diseases such as diabetic neuropathy. The defects in metabolism associated with diabetes could affect the function of these brown adipocytes over time, leading to neuronal damage.

Acknowledgments

We thank Hua Chen from the Vector Development Laboratory at Baylor College of Medicine for vector preparation. This work was supported by grants from the U.S. Department of the Army, Orthopedic Trauma to A.R.D. (DAMD W81XWH-07-1-0214) and E.A.O.-D. (DAMD W81XWH-07-1-0215), a predoctoral fellowship from the American Heart Association (AHA 10805339F) and Kirschstein-NRSA (T32 HL092332-08) to E.A.S, and a postdoctoral fellowship from the National Institute of General Medical Sciences to E.A.S. (K12 GM084897-04).

Author Contributions

E.A.S.: conception and design, collection and assembly of data, data analysis and interpretation, manuscript writing; Z.W.L.: collection and assembly of data, data analysis and interpretation; E.E.U., A.R.D., and E.A.O.-D.: conception and design, data analysis and interpretation, administrative support, manuscript writing, final approval of the manuscript.

Disclosure of Potential Conflicts of Interest

The authors indicate no potential conflicts of interest.

References

1 Seale P, Bjork B, Yang W et al. PRDM16 controls a brown fat/skeletal muscle switch. Nature 2008;454:961–967.

2 Enerbäck S. The origins of brown adipose tissue. N Engl J Med 2009;360:2021–2023.

3 Hondares E, Rosell M, Díaz-Delfín J et al. Peroxisome proliferator-activated receptor α (PPARα) induces PPARγ coactivator 1α (PGC-1α) gene expression and contributes to thermogenic activation of brown fat: Involvement of PRDM16. J Biol Chem 2011;286:43112–43122.

4 Puigserver P, Wu Z, Park CW et al. A cold-inducible coactivator of nuclear receptors linked to adaptive thermogenesis. Cell 1998; 92:829–839.

5 de Jesus LA, Carvalho SD, Ribeiro MO et al. The type 2 iodothyronine deiodinase is essential for adaptive thermogenesis in brown adipose tissue. J Clin Invest 2001;108:1379–1385.

6 Klingenspor M. Cold-induced recruitment of brown adipose tissue thermogenesis. Exp Physiol 2003;88:141–148.

7 Nedergaard J, Golozoubova V, Matthias A et al. UCP1: The only protein able to mediate adaptive non-shivering thermogenesis and metabolic inefficiency. Biochim Biophys Acta 2001;1504:82–106.

8 Cannon B, Nedergaard J. Brown adipose tissue: Function and physiological significance. Physiol Rev 2004;84:277–359.

9 Lowell BB, Spiegelman BM. Towards a molecular understanding of adaptive thermogenesis. Nature 2000;404:652–660.

10 Wilhelm M, Silver R, Silverman AJ. Central nervous system neurons acquire mast cell products via transgranulation. Eur J Neurosci 2005;22:2238–2248.

11 Berger M, Gray JA, Roth BL. The expanded biology of serotonin. Annu Rev Med 2009;60:355–366.

12 Ducy P, Karsenty G. The two faces of serotonin in bone biology. J Cell Biol 2010;191:7–13.

13 Collins S, Yehuda-Shnaidman E, Wang H. Positive and negative control of Ucp1 gene transcription and the role of beta-adrenergic signaling networks. Int J Obes (Lond) 2010; 34(suppl 1):S28–S33.

14 Bartness TJ, Vaughan CH, Song CK. Sympathetic and sensory innervation of brown adipose tissue. Int J Obes (Lond) 2010;34(suppl 1):S36–S42.

15 Harper ME, Green K, Brand MD. The efficiency of cellular energy transduction and its implications for obesity. Annu Rev Nutr 2008;28: 13–33.

16 Garruti G, Ricquier D. Analysis of uncoupling protein and its mRNA in adipose tissue deposits of adult humans. Int J Obes Relat Metab Disord 1992;16:383–390.

17 Olmsted-Davis E, Gannon FH, Ozen M et al. Hypoxic adipocytes pattern early heterotopic bone formation. Am J Pathol 2007;170:620–632.

18 Bartelt A, Bruns OT, Reimer R et al. Brown adipose tissue activity controls triglyceride clearance. Nat Med 2011;17:200–205.

19 Swerdlow RH. Role and treatment of mitochondrial DNA-related mitochondrial dysfunction in sporadic neurodegenerative diseases. Curr Pharm Des 2011;17:3356–3373.

20 Dilling CF, Wada AM, Lazard ZW et al. Vessel formation is induced prior to the appearance of cartilage in BMP-2-mediated heterotopic ossification. J Bone Miner Res 2010; 25:1147–1156.

21 Kopfstein L, Veikkola T, Djonov VG et al. Distinct roles of vascular endothelial growth factor-D in lymphangiogenesis and metastasis. Am J Pathol 2007;170:1348–1361.

22 Mauceri D, Freitag HE, Oliveira AM et al. Nuclear calcium-VEGFD signaling controls maintenance of dendrite arborization necessary for memory formation. Neuron 2011;71:117–130.

23 Salisbury E, Rodenberg E, Sonnet C et al. Sensory nerve induced inflammation contributes to heterotopic ossification. J Cell Biochem 2011;112:2748–2758.

24 Kan L, Lounev VY, Pignolo RJ et al. Substance P signaling mediates BMP dependent heterotopic ossification. J Cell Biochem 2011; 112:2759–2722.

25 Rodenberg E, Azhdarinia A, Lazard ZW et al. Matrix metalloproteinase-9 is a diagnostic marker of heterotopic ossification in a murine model. Tissue Eng Part A 2011;17:2487–2496.

26 Adameyko I, Lallemend F, Aquino JB et al. Schwann cell precursors from nerve innervation are a cellular origin of melanocytes in skin. Cell 2009;139:366–379.

27 Williams JP, Wu J, Johansson G et al. Nf1 mutation expands an EGFR-dependent peripheral nerve progenitor that confers neurofibroma tumorigenic potential. Cell Stem Cell 2008;3:658–669.

28 Nagoshi N, Shibata S, Kubota Y et al. Ontogeny and multipotency of neural crest-derived stem cells in mouse bone marrow, dorsal root ganglia, and whisker pad. Cell Stem Cell 2008;2:392–403.

29 Olmsted-Davis EA, Gugala Z, Gannon FH et al. Use of a chimeric adenovirus vector enhances BMP2 production and bone formation. Hum Gene Ther 2002;13:1337–1347.

30 Fouletier-Dilling CM, Bosch P, Davis AR et al. Novel compound enables high-level adenovirus transduction in the absence of an adenovirus-specific receptor. Hum Gene Ther 2005; 16:1287–1297.

31 Gugala Z, Olmsted-Davis EA, Gannon FH et al. Osteoinduction by ex vivo adenovirus-mediated BMP2 delivery is independent of cell type. Gene Ther 2003;10:1289–1296.

32 Bixby S, Kruger GM, Mosher JT et al. Cell-intrinsic differences between stem cells from different regions of the peripheral nervous system regulate the generation of neural diversity. Neuron 2002;35:643–656.

33 Kreipe H, Heidebrecht HJ, Hansen S et al. A new proliferation-associated nuclear antigen detectable in paraffin-embedded tissues by the monoclonal antibody Ki-S1. Am J Pathol 1993;142:3–9.

34 Künemund V, Jungalwala FB, Fischer G et al. The L2/HNK-1 carbohydrate of neural cell adhesion molecules is involved in cell interactions. J Cell Biol 1988;106:213–223.

35 Nagase T, Nakamura S, Harii K et al. Ectopically localized HNK-1 epitope perturbs migration of the midbrain neural crest cells in Pax6 mutant rat. Dev Growth Differ 2001;43: 683–692.

36 Jungalwala FB. Expression and biological functions of sulfoglucuronyl glycolipids (SGGLs) in the nervous system: A review. Neurochem Res 1994;19:945–957.

37 Yamamoto S, Oka S, Inoue M et al. Mice deficient in nervous system-specific carbohydrate epitope HNK-1 exhibit impaired synaptic plasticity and spatial learning. J Biol Chem 2002;277:27227–27231.

38 Bachman ES, Dhillon H, Zhang CY et al. betaAR signaling required for diet-induced thermogenesis and obesity resistance. Science 2002;297:843–845.

39 Tissir F, Goffinet AM. Reelin and brain development. Nat Rev Neurosci 2003;4:496–505.

40 Lorenzetto E, Panteri R, Marino R et al. Impaired nerve regeneration in reeler mice after peripheral nerve injury. Eur J Neurosci 2008;27:12–19.

41 Cox JS. Disodium cromoglycate (FPL 670) ('Intal'): A specific inhibitor of reaginic antibody-antigen mechanisms. Nature 1967;216: 1328–1329.

42 Yosef N, Xia RH, Ubogu EE. Development and characterization of a novel human in vitro blood-nerve barrier model using primary endoneurial endothelial cells. J Neuropathol Exp Neurol 2010;69:82–97.

43 Morrison SJ, White PM, Zock C et al. Prospective identification, isolation by flow cytometry, and in vivo self-renewal of multipotent mammalian neural crest stem cells. Cell 1999;96:737–749.

44 Joseph NM, Mukouyama YS, Mosher JT et al. Neural crest stem cells undergo multilineage differentiation in developing peripheral nerves to generate endoneurial fibroblasts in addition to Schwann cells. Development 2004; 131:5599–5612.

45 Wu J, Williams JP, Rizvi TA et al. Plexiform and dermal neurofibromas and pigmentation are caused by Nf1 loss in desert hedgehog-expressing cells. Cancer Cell 2008;13:105–116.

46 Kucenas S, Takada N, Park HC et al. CNS-derived glia ensheath peripheral nerves and mediate motor root development. Nat Neurosci 2008;11:143–151.

47 Bunge MB, Wood PM, Tynan LB et al. Perineurium originates from fibroblasts: Demonstration in vitro with a retroviral marker. Science 1989;243:229–231.

48 Fouletier-Dilling CM, Gannon FH, Olmsted-Davis EA et al. Efficient and rapid osteoinduction in an immune-competent host. Hum Gene Ther 2007;18:733–745.

49 Bucelli RC, Gonsiorek EA, Kim WY et al. Statins decrease expression of the proinflammatory neuropeptides calcitonin gene-related peptide and substance P in sensory neurons. J Pharmacol Exp Ther 2008;324:1172–1180.

50 Bronner-Fraser M. Analysis of the early stages of trunk neural crest migration in avian embryos using monoclonal antibody HNK-1. Dev Biol 1986;115:44–55.

51 Dottori M, Gross MK, Labosky P et al. The winged-helix transcription factor Foxd3 suppresses interneuron differentiation and promotes neural crest cell fate. Development 2001;128:4127–4138.

52 Rosen ED, Sarraf P, Troy AE et al. PPAR gamma is required for the differentiation of adipose tissue in vivo and in vitro. Mol Cell 1999;4:611–617.

53 Nedergaard J, Petrovic N, Lindgren EM et al. PPARgamma in the control of brown adipocyte differentiation. Biochim Biophys Acta 2005;1740:293–304.

54 Seale P, Kajimura S, Yang W et al. Transcriptional control of brown fat determination by PRDM16. Cell Metab 2007;6:38–54.

55 Falconer DS. Two new mutants, 'trembler' and 'reeler', with neurological actions in the house mouse (*Mus musculus* L.) J Genet 1951;50:192–205.

56 D'Arcangelo G, Miao GG, Chen SC et al. A protein related to extracellular matrix proteins deleted in the mouse mutant reeler. Nature 1995;374:719–723.

57 Hochstim C, Deneen B, Lukaszewicz A et al. Identification of positionally distinct astrocyte subtypes whose identities are specified by a homeodomain code. Cell 2008;133:510–522.

58 Carmignoto G, Gomez-Gonzalo M. The contribution of astrocyte signalling to neurovascular coupling. Brain Res Rev 2010;63:138–148.

59 Bostrom KI, Garfinkel A, Yao Y et al. Concise review: Applying stem cell biology to vascular structures. STEM CELLS 2012;30:386–391.

60 Clever JL, Sakai Y, Wang RA et al. Inefficient skeletal muscle repair in inhibitor of differentiation knockout mice suggests a crucial role for BMP signaling during adult muscle regeneration. Am J Physiol Cell Physiol 2010;298: C1087–C1099.

61 Bishop GB, Einhorn TA. Current and future clinical applications of bone morphogenetic proteins in orthopaedic trauma surgery. Int Orthop 2007;31:721–727.

62 Riccardi VM. The genetic predisposition to and histogenesis of neurofibromas and neurofibrosarcoma in neurofibromatosis type 1. Neurosurg Focus 2007;22:E3.

See www.StemCellsTM.com for supporting information available online.